University of Kent

Kent Academic Repository

Femerling, Georgette, van Oosterhout, Cock, Feng, Shaohong, Bristol, Rachel M., Zhang, Guojie, Groombridge, Jim J., Gilbert, M. Thomas P. and Morales, Hernán E. (2023) ***Genetic load and adaptive potential of a recovered avian species that narrowly avoided extinction.*** **Molecular Biology and Evolution, 40 (12). ISSN 0737-4038.**

Downloaded from

https://kar.kent.ac.uk/104084/ The University of Kent's Academic Repository KAR

The version of record is available from

https://doi.org/10.1093/molbev/msad256

This document version

Author's Accepted Manuscript

DOI for this version

Licence for this version

UNSPECIFIED

Additional information

Versions of research works

Versions of Record

If this version is the version of record, it is the same as the published version available on the publisher's web site. Cite as the published version.

Author Accepted Manuscripts

If this document is identified as the Author Accepted Manuscript it is the version after peer review but before type setting, copy editing or publisher branding. Cite as Surname, Initial. (Year) 'Title of article'. To be published in ***Title of Journal*** , Volume and issue numbers [peer-reviewed accepted version]. Available at: DOI or URL (Accessed: date).

Enquiries

If you have questions about this document contact ResearchSupport@kent.ac.uk. Please include the URL of the record in KAR. If you believe that your, or a third party's rights have been compromised through this document please see our Take Down policy (available from https://www.kent.ac.uk/guides/kar-the-kent-academic-repository#policies).

Genetic load and adaptive potential of a recovered avian species that narrowly avoided extinction

Georgette Femerling[1,2.10], Cock van Oosterhout[3], Shaohong Feng[4,5,6], Rachel M. Bristol[7,8], Guojie Zhang[4,5,6], Jim Groombridge[8], M. Thomas P. Gilbert[1,9] and Hernán E. Morales[1*]

[1]Globe Institute, Faculty of Health and Medical Sciences, University of Copenhagen, Copenhagen, Denmark

[2] Centro de Ciencias Genómicas, Universidad Nacional Autónoma de México, Cuernavaca, México

[3]School of Environmental Sciences, University of East Anglia, Norwich, UK

[4]Center for Evolutionary & Organismal Biology, Zhejiang University School of Medicine, Hangzhou, China

[5]Liangzhu Laboratory, Zhejiang University Medical Center, 1369 West Wenyi Road, Hangzhou, China

[6]Innovation Center of Yangtze River Delta, Zhejiang University, Jiashan, China

[7]La Batie, Beau Vallon, Mahe, Seychelles

[8]Durrell Institute of Conservation and Ecology, School of Anthropology and Conservation, Division of Human and Social Sciences, University of Kent, Canterbury, Kent, CT2 7NR, United Kingdom.

[9]University Museum, NTNU, Trondheim, Norway

[10]Department of Human Genetics, McGill University, Montreal, Quebec, Canada

* Corresponding author - Hernán E. Morales (hernanm [at] sund.ku.dk)

Abstract

High genetic diversity is a good predictor of long-term population viability, yet some species persevere despite having low genetic diversity. Here we study the genomic erosion of the Seychelles paradise flycatcher (*Terpsiphone corvina*), a species that narrowly avoided extinction after having declined to 28 individuals in the 1960s. The species recovered unassisted to over 250 individuals in the 1990s and was downlisted from Critically Endangered to Vulnerable in the IUCN Red List in 2020. By comparing historical, pre-bottleneck (130+ years old) and modern genomes, we uncovered a 10-fold loss of genetic diversity. Highly deleterious mutations were partly purged during the bottleneck, but mildly deleterious mutations accumulated. The genome shows signs of historical inbreeding during the bottleneck in the 1960s, but low levels of recent inbreeding after demographic recovery. Computer simulations suggest that the species long-term small N_e reduced the masked genetic load and made the species more resilient to inbreeding and extinction. However, the reduction in genetic diversity due to the chronically small N_e and the severe bottleneck is likely to have reduced the species adaptive potential to face environmental change, which together with a higher load,

© The Author(s) 2023. Published by Oxford University Press on behalf of Society for Molecular Biology and Evolution. This is an Open Access article distributed under the terms of the Creative Commons Attribution License (https://creativecommons.org/licenses/by/4.0/), which permits unrestricted reuse, distribution, and reproduction in any medium, provided the original work is properly cited.

ACCEPTED MANUSCRIPT

Downloaded from https://academic.oup.com/mbe/advance-article/doi/10.1093/molbev/msad256/7442647 by University of Kent user on 27 November 2023

compromises its long-term population viability. Thus, small ancestral N_e offers short-term bottleneck resilience, but hampers long-term adaptability to environmental shifts. In light of rapid global rates of population decline, our work show that species can continue to suffer the effect of their decline even after recovery, highlighting the importance of considering genomic erosion and computer modelling in conservation assessments.

Introduction

Global population abundance of 4,392 species monitored over the last 40 decades has declined by 68% (Almond et al. 2022), threatening their long-term viability. On the IUCN Red List, 33,777 species (47.4%) are facing population decline, compared to 36,264 (50.9%) with stable population size, and 1274 (1.8%) that are increasing in size (IUCN 2022). A growing number of species are being classified as threatened with extinction, i.e., in the Red List categories of Vulnerable, Endangered, or Critically Endangered (Monroe et al. 2019). On the other hand, effective conservation management has been able to recover the population size after a severe bottleneck for a small number of species, resulting in their downlisting on the IUCN Red List (e.g., the snow leopard, the giant panda and the pink pigeon; (Mallon and Jackson 2017; Swaisgood et al. 2018). However, even when effective conservation actions are capable of reverting population declines, the negative genetic effects that may arise during population declines can persist (Kuussaari et al. 2009; Tilman et al. 1994). Populations that have recovered from a bottleneck could be subjected to a genetic drift debt where they continue to lose genetic diversity, even after demographic recovery (Gilroy et al. 2017; Pinto et al. 2023). Population decline generates genetic drift and inbreeding that erode genetic diversity, compromising the viability of wild populations (Bozzuto et al. 2019; Lande and Shannon 1996; Lynch et al. 1995; Willi et al. 2006). Thus, investigating the evolutionary genomic consequence of population decline in species that have collapsed, but recovered and avoided extinction, improves our understanding of the extinction risk, recovery potential, and the long-term viability of threatened populations.

Empirical and simulation studies have shown that population bottlenecks and long-term small effective population sizes (N_e) could be conducive to the reduction of deleterious variation through the purging of deleterious mutations (Dussex et al. 2021; Garcia-Dorado 2012; Grossen et al. 2020; Hedrick and Garcia-Dorado 2016; Khan et al. 2021; Kleinman-Ruiz et al. 2022; Kyriazis et al. 2021; Pérez-Pereira et al. 2021; van Oosterhout et al. 2022). Theoretically, this could make species more robust to inbreeding depression. However, small population sizes

ACCEPTED MANUSCRIPT

Downloaded from https://academic.oup.com/mbe/advance-article/doi/10.1093/molbev/msad256/7442647 by University of Kent user on 27 November 2023

may also increase the genetic load through the accumulation of mildly deleterious mutations (Bertorelle et al. 2022; Grossen et al. 2020; Smeds and Ellegren 2022). Furthermore, genetic drift in small populations leads to reduced adaptive potential in the face of environmental change (Willi et al. 2006). At present, we have an incomplete understanding of the short- and long-term consequences of population decline and small effective population size on the viability and extinction risk of species (Forester et al. 2022; Hedrick and Garcia-Dorado 2016; Mable 2019).

The rate of genomic erosion and its impact on extinction probability is a complex outcome of the interaction between long-term trends of N_e, recent population decline, the response of different types of genetic variation (e.g., deleterious mutations and adaptive genetic variation), and the rate of environmental change. Here, we quantify the genomic erosion in the Seychelles paradise flycatcher (*Terpsiphone corvina*), a species whose population declined to 28 individuals in 1965, followed by an (unassisted) recovery to over 250 individuals by the year 2000. Additionally, in 2008 a self-sustaining, growing population was established on Denis Island with translocated individuals. After these demographic gains, the species' conservation status in the IUCN Red List was downlisted from Critically Endangered to Vulnerable (IUCN 2022/1). We directly compare genomic variation pre- and post-population decline by sequencing whole genomes of museum-preserved samples (>130 years old) and modern samples. We show that the species suffered a 10-fold decline in genome-wide genetic diversity, one of the largest losses compared to other birds with reported historical comparisons. This decline has left the modern Seychelles paradise flycatcher population with a lower genome-wide diversity compared to many other Endangered and Critically Endangered bird species. We used individual-based genomic simulations to investigate how the Seychelles paradise flycatcher managed to avoid extinction after suffering such a drastic population decline and loss of genetic diversity. Our results indicate that the ancestral, pre-bottleneck population had a low masked genetic load due to their long-term small Ne. This effect was conducive to less inbreeding depression that allowed them to avoid extinction and successfully recover. However, we also show that this long-term small Ne, together with the substantial genetic diversity loss, have likely reduced the species' adaptive potential and jeopardised their long-term viability when faced with environmental change.

ACCEPTED MANUSCRIPT

Downloaded from https://academic.oup.com/mbe/advance-article/doi/10.1093/molbev/msad256/7442647 by University of Kent user on 27 November 2023

Results

Population structure and genetic diversity

We analysed the population genomics of the Seychelles paradise flycatcher, comparing 13 historical samples (coverage: mean = 4.7 sd = 1) and 18 modern samples (coverage: mean = 9.2 sd = 0.4). Historical and modern samples (Fig. 1A) showed a pattern of strong genetic differentiation (PC1; 29% explained variance), with the modern samples forming a homogenous group, and the historical samples differentiated between islands (PC2; 5% explained variance) (Fig. 1B). The rest of the PCs mostly account for the variation within the historical populations (Fig. S1). The admixture analysis assuming three genetic groups (K=3) reflects the strong differentiation between historical and modern individuals and the geographical structure within the historical individuals (Fig. S2). Higher Ks yielded no clear signal of co-ancestry between the historical and modern La Digue individuals. This failure to retrieve a historical component in the modern samples is likely due to strong genetic drift changing the allele frequencies in the modern population (Ebenesersdóttir et al. 2018).

On average, the global individual heterozygosity of modern individuals (La Digue: mean=0.00024, sd=0.00002) was 6.4 times lower than that of the historical individuals (La Digue: mean=0.00162, sd=0.0003 and Praslin: mean=0.00157, sd=0.0002) (Fig. 1C). A genomic sliding-window analysis of population pairwise nucleotide diversity shows that the loss with this metric was 10.9-fold, and that genetic diversity was lost similarly throughout the entire genome (Fig. 1D). Similar comparisons in different bird species have reported smaller losses in nucleotide diversity: the crested ibis and the Chatham Island black robin with a 1.8-fold loss (Feng et al. 2019; von Seth et al. 2022), or in heterozygosity levels: the New Zealand Saddleback, 4.16-fold (Taylor et al. 2007); the Mangrove Finch: 1.32-fold (Lawson et al. 2017); Greater Prairie Chicken: 1.26-fold (Bellinger et al. 2003) (Supplementary Table 2). The resulting extremely low genetic diversity in the modern population of the Seychelles paradise flycatcher is considerably lower compared to many other threatened bird species (Fig. S3). Our results highlight how even when a population has recovered demographically, it can still be a long way away from recovering in terms of genetic diversity. The results are robust to the difference of depth between modern and historical samples, as all the metrics hold the same pattern when modern samples were down sampled to the same mean depth of coverage of the historical samples (Figs. S4-S7). Moreover, ultra-conserved regions of the genome exhibited reduced diversity compared to non-conserved regions in historical samples, but after the population collapse all regions show the pronounced diversity loss (Fig. S8), providing further evidence of

ACCEPTED MANUSCRIPT

Downloaded from https://academic.oup.com/mbe/advance-article/doi/10.1093/molbev/msad256/7442647 by University of Kent user on 27 November 2023

the same extreme effect of the bottleneck. At the same time, the amount of diversity observed in ultra-conserved regions could reflect some moderate effect of DNA damage inflating historical diversity estimates. Therefore, it is important to keep in mind that despite following strict filtering steps and performing several checks (see Methods and Fig S9-S13), biases inherit to the analysis of historic DNA cannot be ruled out completely. In particular, the magnitude of diversity loss could be slightly overestimated.

Demography and runs of homozygosity

The modern La Digue population has a skewed distribution towards shorter (<5Mb) Runs of Homozygosity (ROHs) (Fig. 2A). Longer ROHs would be expected if closely related individuals mated with each other within the last 10 generations (Fig. 2B; Fig. S15). Hence, the distribution skewed towards shorter ROH length suggests an absence of recent inbreeding in our data (F_{ROH} < 0.01; Fig. 2B). ROHs that are 1-2 Mb long (Fig. 2A) are expected to have been formed 10-20 generations ago (Fig. S15), which is consistent with historical inbreeding around the year 1974 (F_{ROH} = 0.2-0.4), and it is likely to be a product of the bottleneck that started in the mid-1960s (Fig. 2B).

In agreement with the F_{ROH} evidence, the reconstructed recent demographic history (within the last 100 generations) with GONE (Santiago et al. 2020) also recovered a clear signature of the bottleneck by registering a dramatic drop in the N_e around the year 1975 (~17 generations ago; Fig. 2C), The PSMC (Li and Durbin 2011) reconstruction shows a very large ancient population that decreased in size and remained small for the last 10,000 years (Fig. 2D). It is important to note that the deep demographic history reconstruction with PSMC carries some uncertainty. The maximum N_e=530,635 estimated at ~55,000 years substantially exceeds the current carrying capacity of the entire Seychelles archipelago. However, past sea levels were highly dynamic, connecting and disconnecting islands in the archipelago on at least 14 separate occasions (Ali 2018; Ryan et al. 2009; Warren et al. 2010). Thus, it is possible that the ancient population could have been much larger at times of increased island connectivity. Seychelles' landmass is estimated to have been up to 180 times its present size, and gene flow may have been facilitated by islands in the western Indian Ocean that could have acted as stepping-stones between landmasses during the Pliocene and Pleistocene (Cheke and Hume 2008; Warren et al. 2010). This geological signature has been seen in other Seychelles taxa (Groombridge et al. 2002; Labisko et al. 2022; Rocha et al. 2013). However, the large ancestral N_e can also be an artefact of population structure, selection and admixture, all of which are known to introduce biases to coalescent demographic reconstruction (Boitard et al. 2022; Johri

ACCEPTED MANUSCRIPT

Downloaded from https://academic.oup.com/mbe/advance-article/doi/10.1093/molbev/msad256/7442647 by University of Kent user on 27 November 2023

et al. 2021; Mazet et al. 2016). For example, if island populations were reproductively separated at some point, PSMC estimates would be inflated as alleles would not coalesce. Irrespective of the uncertainty of ancient N_e estimates, we can be confident that the relatively-recent genetic lineage remained small for at least 5,000 generations (10,000 years), in agreement with a history of long-term small N_e.

Genetic load analyses

We next compared the temporal changes in putative deleterious mutations. Given the massive amount of genetic diversity loss in the modern population (Fig. 2), many deleterious alleles are likely to have been lost due to genetic drift during the bottleneck. However, a few mutations could have drifted to higher frequency because of less efficient purifying selection in the small-N_e population. Therefore, to examine the impact of genetic drift and purifying selection on deleterious variation that remained in the modern population, we conservatively focused on (putative) deleterious alleles that were observed in at least one historical and one modern individual. Mutations classified as synonymous (nearly-neutral) and missense (mildly deleterious) exhibited an increased frequency in the modern samples compared to the historical sample, but those classified as loss-of-function (LoF; highly deleterious) exhibited a reduced frequency (Fig. 3A). Next, we counted derived (putatively) deleterious alleles for missense and LoF categories, corrected by the count of derived synonymous alleles. Modern samples showed higher derived counts of missense alleles (Fig. 3B), and also higher counts of homozygous derived missense alleles (Fig. 3C). Although there was no significant change in the counts of LoF alleles (Fig. 3B), the count of homozygous derived LoF alleles went slightly down in the modern samples (Fig. 3C). Altogether, these findings show that severely deleterious (LoF) mutations have been reduced by purifying selection during the bottleneck, although this effect was weak and only affected the load of homozygous LoF mutations. It is important to consider the effect of stringent filtering in temporal analysis involving historic DNA. Only retaining deleterious alleles that were observed both in the historical and modern individuals impaired our ability to detect the full extent of purifying selection on deleterious variation, in particular the effect of purging. While this filtering step is needed to reduce the potential bias caused by sequencing artifacts of historical samples and other sequencing errors, it is a duly conservative approach with a considerable downside. Specifically, it prevented us from finding LoF mutations that are expected to be present in at very low frequencies in the ancestral population (Dussex et al. 2023), but which are no longer present in the modern population. Per definition, by using this stringent filtering step, it became technically impossible to detect purging (i.e., the complete

ACCEPTED MANUSCRIPT

Downloaded from https://academic.oup.com/mbe/advance-article/doi/10.1093/molbev/msad256/7442647 by University of Kent user on 27 November 2023

removal of harmful variants due to purifying selection). On the other hand, other classes of mutations escaped the effect of purifying selection due to the strong genetic drift, resulting in the increase of nearly-neutral (synonymous) and mildly deleterious (missense) mutations.

Individual-based simulations

We assessed how different types of genomic variation (deleterious variation and adaptive variation) respond to the population decline and recovery in the species by simulating historical populations with small (1X), medium (5X), and large (10X) ancestral population size (Fig. 4A). The total ancestral deleterious variation (i.e., genetic load = sum of masked load plus realised load) scales positively with population size (Fig. 4B). Historically, most deleterious variation is in the form of masked load (Fig. 4C) (i.e., these mutations do not reduce fitness), and only a small proportion is part of the realised load (Fig. 4D) (i.e., mutations that reduce fitness). During the population size collapse, there is a marginal reduction of the genetic load (Fig. 4B) as many rare, low-frequency variants are randomly lost after the bottleneck, and other (mostly high-impact) variants are purged by purifying selection.

On the flip side, during the bottleneck, some of the masked load is converted into realised load by inbreeding (Fig. 4C and D), and this conversion results in a loss of fitness (i.e., inbreeding depression). Two processes are at play here. First, whilst most deleterious variants are lost, genetic drift increases the frequency of a small number of deleterious mutations. Given their now elevated frequency, these deleterious mutations are more likely to be found in homozygous genotypes. Second, the bottleneck increases the probability of mating between closely related individuals. By increasing homozygosity, both genetic drift and inbreeding convert the masked load into a realised load. Figure 4D illustrates this in computer simulations. During the population size collapse, the realised load of the largest ancestral population is increased to around 0.2 lethal equivalents, which equates to a fitness $w = e^{-0.2} = 0.82$. For the smallest ancestral population size on the other hand, population size collapse increases the realised load to circa 0.1 lethal equivalents, which equates to $w = e^{-0.1} = 0.90$. In other words, individuals in large ancestral populations suffer from more severe inbreeding depression during population size collapse than individuals derived from historically small populations (Kyriazis et al. 2021; Mathur and DeWoody 2021; van Oosterhout et al. 2022).

During population recovery the compositions of the genetic load changed substantially (Fig. 4 B-D). After having experienced the effect of the bottleneck for longer, the realised load peaked at over 0.4 lethal equivalents for the largest ancestral population size. Severe inbreeding depression during this stage would have reduced the fitness of individuals markedly,

ACCEPTED MANUSCRIPT

Downloaded from https://academic.oup.com/mbe/advance-article/doi/10.1093/molbev/msad256/7442647 by University of Kent user on 27 November 2023

$w = e^{-0.4} = 0.67$ (i.e., 33% individual fitness loss in average). Figure 4D shows that the worst affected individuals express a realised load of 0.8 lethal equivalents, which means that their fitness would be less than half that of their pre-bottleneck ancestors. In contrast, the smallest ancestral population (i.e., the simulations most similar to the Seychelles paradise flycatcher's historical demography) suffer much less inbreeding depression at this point. An average individual is expected to express 0.2 lethal equivalents, a ~18% reduction in fitness. This explains why the small population has a lower extinction risk (Fig. 4E), and why the Seychelles paradise flycatcher may have avoided extinction. After recovery, natural selection regains power in an expanding population and the realised load is once more selected against, reducing the genetic load (Fig. 4D).

In the same models we also simulated adaptive variation as additive genetic variants. Unlike unconditionally deleterious mutations (i.e. the genetic load) that always reduce fitness when expressed, additive genetic variants can either increase or decrease fitness depending on the genetic background and the environment (Charlesworth 2013a; Charlesworth 2013b). Figure 4F shows that the amount of additive genetic variation (V_a) increases with the ancestral population size. In a stable environment, ancestrally larger populations have on average lower fitness (Fig. 4G). This is because they contain more segregating variants which can produce more extreme (i.e., suboptimal) phenotypes (Charlesworth 2013b). However, their larger V_a gives them a wider phenotypic breath and a greater adaptive potential when environmental conditions change. As expected, population size collapse reduces V_a, but as with the genetic load, the effect on quantitative genetic variation is most pronounced during recovery (Fig. 4F). Remarkably, the loss in V_a results in the most pronounced fitness loss in large ancestral populations. However, after environmental change, recovered populations derived from large ancestral populations can better match the new environmental optimum. Their superior adaptive potential ensures that such populations have a higher fitness during environmental change in the future (Fig. 4G).

Discussion

We analysed the whole genome sequence data of a threatened species that suffered a population decline to 28 individuals, the Seychelles paradise flycatcher (*Terpsiphone corvina*), comparing the level of genomic erosion between 13 historic (> 130-years-old) and 18 modern birds. In addition, we conducted computer simulations to study the effects of population decline and recovery on the genetic load and adaptive evolutionary potential. We thus assessed the

ACCEPTED MANUSCRIPT

Downloaded from https://academic.oup.com/mbe/advance-article/doi/10.1093/molbev/msad256/7442647 by University of Kent user on 27 November 2023

long-term impacts of changes in genomic variation on population viability. We uncovered a 10-fold loss of genetic diversity in the Seychelles paradise flycatcher, reflecting severe genetic drift during population size decline that continues to act despite population recovery. We also found evidence of historical inbreeding at the time of population decline, but no evidence of recent inbreeding, reflecting successful population recovery. Demographic reconstructions suggest that prior to its recent population decline, the Seychelles paradise flycatcher sustained a small effective population size (N_e) for thousands of generations. Our genomic simulations suggest that this reduced the amount of (masked) genetic load in the ancestral population, resulting in only mild inbreeding depression during its collapse. In other words, the long-term small N_e of this species may have allowed for its (unassisted) demographic recovery and helped avoid extinction. However, the species has not recovered its genetic diversity, and the mean fitness of individuals is predicted to be lower than that of their ancestors. Our simulations also indicate that the loss of genetic diversity has likely reduced their adaptive potential, and this reduction could jeopardise the species' long-term viability when faced with environmental change. Our analyses illustrate the power of historical vs. modern comparisons, in combination with analyses of genomic erosion and simulations to assess the medium to long-term effects of population decline and recovery on population viability (Díez-del-Molino et al. 2018; Dussex et al. 2021; Feng et al. 2019; Sánchez-Barreiro et al. 2021). Importantly, we showcase how to use this integrative approach to inform conservation assessments (Jensen et al. 2022; van Oosterhout et al. 2022).

Historical inbreeding, but not recent inbreeding

Remarkably, we did not find evidence of long runs of homozygosity (ROH), which are typically observed in recently bottlenecked species such as the crested Ibis (Feng et al. 2019), the alpine ibex (Grossen et al. 2020), the white rhinoceros (Sánchez-Barreiro et al. 2021), and different horse breeds (Grilz-Seger et al. 2018). Instead, we found that the most common category of ROHs was between 1-2 Mb long. ROHs are formed when closely related individuals mate (i.e., consanguineous mating or inbreeding). The inbred offspring inherit identical segments of DNA, which show up as ROH across the genome. If this offspring mates with unrelated individuals in later generations, the ROHs can be "broken down" by recombination and they become shorter. Thus, the distribution of ROH size reflects an inbreeding timeline. Our results suggest that the population decline imposed severe inbreeding, and that at the time of the bottleneck individuals had ~40% of their genomes contained in ROHs (F_{ROH}=0.4; Fig. 2B). Upon demographic

ACCEPTED MANUSCRIPT

Downloaded from https://academic.oup.com/mbe/advance-article/doi/10.1093/molbev/msad256/7442647 by University of Kent user on 27 November 2023

recovery, ROHs were broken down by recombination, leaving this signature of relatively shorter ROHs (1-2 Mb), consistent with historical inbreeding (~45 years ago).

The lack of long ROHs, on the other hand, indicates the absence of recent inbreeding (F_{ROH}<0.01 in the last decade; Fig. 2B), meaning that the demographic recovery allowed the Seychelles paradise flycatcher to avoid consanguineous mating. Even though pairs of Seychelles paradise flycatchers normally retain the same territory for life and are socially monogamous, their rate of extra-pair paternity is very high, with 71% of chicks being the biological offspring of males from different territories across the island (Bristol 2014). This could explain why once the population recovered demographically it was able to avoid inbreeding.

Genetic load, adaptive potential, and extinction risk

Consistent with theoretical expectations (Bertorelle et al. 2022; Hedrick and Garcia-Dorado 2016; Santiago et al. 2020; Dussex et al. 2023), and empirical observations in other taxa (Dussex et al. 2021; Grossen et al. 2020; Khan et al. 2021; Kleinman-Ruiz et al. 2022; Pérez-Pereira et al. 2021; Robinson et al. 2022), we observed a distinct pattern for highly deleterious and mildly deleterious variation after the bottleneck. It is important to note that we focused solely on deleterious alleles that remained in the modern population. This minimised the bias caused by sequencing artifacts typical in the analysis of historical samples. Furthermore, many deleterious variants have been removed during the bottleneck, and we are interested in analysing the fate of the remaining genetic load of segregating mutations. Theory predicts that population bottlenecks reduce the number of segregating sites with deleterious mutations, but also that they increase the frequency of deleterious variants at some loci that survive the bottleneck (Dussex et al. 2023). This elevated frequency increases the level of homozygosity, which increases the realised load and leads to inbreeding depression (Bertorelle et al. 2022; Hedrick and Garcia-Dorado 2016; Santiago et al. 2020). In turn, this allows for purifying selection to reduce some of the realised load. We observed only marginal evidence for purifying selection on highly-deleterious variants, i.e., the loss-of-function (LoF) mutations. The genetic load of homozygous LoF mutations decreased slightly after the bottleneck. These variants have the strongest fitness effects and are thus most effectively removed by selection during inbreeding. On the other hand, derived alleles of mildly deleterious variants (i.e., missense mutations) increased in frequency and count. This is because purifying selection is less efficient in populations with a small effective size. During population decline, inbreeding and genetic drift convert the masked load into realised load (e.g., Mathur and DeWoody 2021; Smeds and Ellegren 2022). Because of the reduced efficacy of purifying selection, a portion of the

ACCEPTED MANUSCRIPT

Downloaded from https://academic.oup.com/mbe/advance-article/doi/10.1093/molbev/msad256/7442647 by University of Kent user on 27 November 2023

converted load escaped selection and persisted as realised load, reducing population viability (Grossen et al. 2020; van Oosterhout et al. 2022; Pinto et al. 2023).

Small-island species with long-term small N_e accumulate less masked load compared to mainland species with large ancestral N_e. Such species will have less segregating masked genetic load to be converted into realised load during a bottleneck, particularly from highly deleterious variants (Dussex et al. 2033). Therefore, this could make small-island species more resilient to the effects of strong inbreeding depression during population decline, although mild inbreeding depression could still operate. Possibly this could also explain why we observe a modest effect of purifying selection on the LoF variation. Our reconstruction of the recent demographic history of the Seychelles paradise flycatcher is consistent with a scenario in which prior to the recent bottleneck of 1964, the species had a long-term small N_e for the last ~5,000 generations. Given that historically large populations possess a high masked load, they are particularly prone to the detrimental effects of load conversion during population size collapse (Mathur and DeWoody 2021; van Oosterhout et al. 2022). Conversely, the Seychelles paradise flycatcher was particularly resilient to inbreeding depression and this likely played a role in their successful (unassisted) demographic recovery. This hypothesis of long-term reduction of the genetic load in the Seychelles paradise flycatcher is consistent with the observed signal of historical population structure between islands, also observed by Bristol et al. (2013), which used microsatellites for more historical samples distributed across multiple islands. This could have been conducive to effective long-term reduction of deleterious variation as selection operated on small ancestral populations with little inter-island gene-flow.

The Seychelles paradise flycatcher population size has been steadily increasing in the past 20 years. Nonetheless, even after the apparent demographic recovery, the modern population possesses a very low genetic diversity. This is of conservation concern because genome-wide diversity is an important predictor of population fitness and adaptive potential (Fagan and Holmes 2006; Hansson and Westerberg 2002; Harrisson et al. 2014; Mathur and DeWoody 2021; Kardos et al. 2021; Willi et al. 2006; Willi et al. 2022; Willoughby et al. 2015). Our computer simulations show the loss of genetic diversity may lead to reduced adaptive response during environmental change. In turn, and opposite to the prediction for the genetic load, this could elevate its extinction risk compared to populations with a larger ancestral N_e (Lande and Shannon 1996; Willi et al. 2006). In summary, the long-term small ancestral N_e represents a trade-off in which populations might be more resilient on the short-term when facing strong bottlenecks, but less resilient on the long-term in the face of environmental change.

ACCEPTED MANUSCRIPT

Downloaded from https://academic.oup.com/mbe/advance-article/doi/10.1093/molbev/msad256/7442647 by University of Kent user on 27 November 2023

The role of genomics in species conservation assessments

The incorporation of genetic information into assessments of conservation status and policy remains inadequate (Hoban et al. 2020; Laikre et al. 2020). Here, we show the impact of genomic erosion in the Seychelles paradise flycatcher, a species that has made a successful demographic recovery that resulted in its downlisting in the IUCN Red List of Threatened Species. Our findings suggest that its ancestrally small N_e might have conferred resilience to inbreeding that initially eases demographic recovery. However, it may also compromise its adaptive potential, particularly during environmental change. Moreover, it is important to note that the reduction of their ancestral genetic load happened (naturally) over thousands of generations. In addition, the chronic reduction in fitness caused by an elevated realised load is likely to put the species at increased risk of extinction. This might be of particular relevance to other island endemic species, which are, for example, characterised by reduced immune function, partially due to their low N_e (Barthe et al. 2022). Accordingly, low genetic diversity can make species more prone to emerging infectious diseases and interspecific competition, which is a substantial risk given the high rates of new colonisations and invasive species in islands (Lockwood et al. 2009; Sax and Gaines 2008). Our work demonstrates the power of direct comparisons between historical and modern whole genomes to reconstruct the temporal dynamics of diversity, demography and inbreeding, and the importance of combining these insights with simulations to inform conservation. We argue that the downlisting of the IUCN Red List status may sometimes be premature and species assessments should include assessment of the risks posed by genomic erosion. A promising way forward to achieve this is incorporating the analysis of genomic erosion in population viability analysis (PVA) with novel computer simulations methods to leverage the full power of genomic and ecological/demographic data.

Methods

Study system and sampling

The Seychelles paradise flycatcher historically inhabited five islands in the Seychelles archipelago. In the early 1900s, the species disappeared from three islands (Aride, Felicité, and Marianne) and in the 1980s disappeared from a fourth one (Praslin). Restricted to a single island (La Digue) in 1965 the population size was reduced to 28 individuals. By the year 2000, the population recovered to ~250 individuals, relatively unassisted. In the year 2008, 23 individuals from La Digue were introduced to Denis Island and successfully established (Henriette and

ACCEPTED MANUSCRIPT

Downloaded from https://academic.oup.com/mbe/advance-article/doi/10.1093/molbev/msad256/7442647 by University of Kent user on 27 November 2023

Laboudallon 2011). These populations continue to grow without assistance, with a current estimated species census population size of 350 – 506 individuals (IUCN 2022/1).

A previous study of historical vs. modern diversity using 14 microsatellites reported a significant reduction in heterozygosity after the bottleneck (Bristol et al. 2013). Following Bristol et al. (2013), we sampled 13 historical individuals collected between 1877 to 1888, and 19 modern individuals collected between 2007 and 2008 (Supplementary table 1; Fig. 1A). Historical samples were sourced from natural history collections as small (2-4 mm) pieces of toe-pad. Information about preservation methods is generally not available for old samples, however, bird toe-pads are often a good source of endogenous DNA. This is because their preservation method, which normally involves natural drying, is less harmful compared to the arsenic and formalin treatments commonly used elsewhere (Tsai et al. 2020).

Genomic libraries and sequencing

Historical DNA extractions were carried out with a modified version of Campos & Gilbert (2012) in a PCR-free clean laboratory exclusively designated for ancient DNA. Historical single-stranded sequencing libraries were prepared following the Santa Cruz Reaction protocol (Kapp et al. 2021), as modified for the DNBSEQ-G400 sequencing platform (van Grouw et al. in review) and amplified in three indexed PCR reactions. Modern DNA extractions were done with the DNAeasy commercial kit (Qiagen) following the manufacturer's recommendations and directly submitted to BGI Copenhagen for sequencing in their DNBSEQ-G400 platform.

Sample processing

We assessed the quality of the raw sequencing reads by running FastQC (Andrews, 2010) and summarised the results with MultiQC (Ewels et al. 2016). We then mapped the sequencing reads to the publicly available *de novo* sequenced reference genome of the Seychelles paradise flycatcher produced by the B10K consortium (Zhang et al. 2015), available at https://b10k.scifeon.cloud/#/b10k/Sample/S15237). We ran the automated pipeline PALEOMIX (Schubert et al. 2014) per sample for both the historical and the modern datasets. This pipeline carries out the pre-processing steps of removing adapters and collapsing mate reads, read mapping with BWA (Li and Durbin 2010), and quantifies the post-mortem damage of historical samples by running MapDamage (Ginolhac et al. 2011) (see Fig. S16-S17 for results). We employed the *aln* algorithm with default parameters for mapping historical samples ignoring reads shorter than 30 bp. This algorithm has shown good performance for short and damaged reads (Schubert et al. 2012), moreover this is the recommended BWA algorithm for reads

ACCEPTED MANUSCRIPT

Downloaded from https://academic.oup.com/mbe/advance-article/doi/10.1093/molbev/msad256/7442647 by University of Kent user on 27 November 2023

shorter than 70 bp (Li and Durbin 2010). We employed the *mem* algorithm for modern samples as it is the recommended BWA algorithm for reads longer than 70 bp and represents considerable gains on speed (Li and Durbin 2010). Duplicates were removed with picard MarkDuplicates (Broad Institute, 2018) and InDels were realigned with GATK (Van der Auwera and O'Connor 2020). We estimated the percentage of endogenous content by computing the rate between uniquely mapped reads and total reads. On average, historical samples had an endogenous content of 57.26% (sd. 4.00%), and modern samples of 96.23% (sd.1.86%; table S1). A summary of additional read and mapping statistics, as well as sample metadata, can be found in table S1.

We performed a depth-based analysis to identify and remove sex chromosome-derived scaffolds following Pečnerová et al. (2021) as their sex-biased pattern of inheritance can bias genetic diversity estimates. Considering that females are the heterogametic sex in birds (ZW), we calculated the difference in the normalized average depth between males and females, expecting that coverage will be nearly double in males relative to females for the Z chromosome, and absent in males but present in females for the W chromosome. In total, 1308 potential sex-linked scaffolds were removed from the subsequent analyses (73.4 Mb putatively Z-linked and 10.7 Mb putatively W-linked).

The small population size and population structuring can result in the sampling of closely related individuals which would inflate the estimated level of inbreeding. To avoid this, we identified and removed closely related individuals using NGSrelate2 (Hanghøj et al. 2019). We used a threshold of KING >= 0.25, R0 <= 0.1 and R1 >= 0.5 as described in Waples et al. (2019). We found only one closely related pair in the modern dataset, and we removed one of these individuals from the final dataset (Fig. S18). The pedigree metadata confirmed these two individuals had a parent-offspring relationship.

Historical DNA biases

Historical DNA is subject to post-mortem DNA damage and contamination. This commonly leads to short sequencing reads that are error-prone and have lower quality, and samples that have low endogenous content and a low depth of coverage. We took several steps to counteract these challenges. First, we confirmed that two common features of ancient DNA datasets: reduced average sequence lengths and low coverage, did not generate reference genome mapping biases (Gopalakrishnan et al. 2022) in our historical dataset (Fig. S9). Second, we used dedicated software for low-coverage samples, ANGSD 0.921 (Korneliussen et al. 2014), to estimate genotype likelihoods and avoid directly calling genotypes. Across all

ACCEPTED MANUSCRIPT

Downloaded from https://academic.oup.com/mbe/advance-article/doi/10.1093/molbev/msad256/7442647 by University of Kent user on 27 November 2023

ANGSD methods, we used the GATK algorithm, filtered for a base quality of 20 and a mapping quality of 30. For each population or group of samples, we computed the 1 and 99% quantiles of global depth to filter out regions with extremely low and extremely high depth. For SNP calling we inferred the major and minor alleles and used the likelihood test with a p-value threshold of $1x10^{-6}$. Third, as commonly done in ancient DNA analyses to counteract biases from post-mortem DNA damage, we removed transitions for all analyses that compared historical and modern samples. Finally, we confirmed that our finding that the modern population lost a considerable part of its genetic diversity was not heavily biased by the low quality of historical reads by comparing the loss of diversity across the genome (Fig. S10) against mapping quality (Fig. S11), average depth (Fig. S12), and DNA damage (Fig. S13).

Population structure and genetic diversity

We performed a Principal component Analysis with PCAngsd 1.01 (Meisner and Albrechtsen 2018) with the genotype likelihoods of the joint historical-modern dataset. Next, we estimated their admixture proportions with NGSAdmix (Skotte et al. 2013), running 250 independent runs from K=2 to K=6. We evaluated the different runs using EvalAdmix (Garcia-Erill and Albrechtsen 2020) and estimated the best K using Clumpak Best K algorithm (Kopelman et al. 2015). We visualised the proportions using PONG (Behr et al. 2016).

Per-sample global heterozygosity estimates were computed directly from the site frequency spectrum (SFS) of each sample by calculating the genome-wide proportion of heterozygous genotypes. We first computed the site allele frequency (SAF) per sample in ANGSD, followed by the realSFS function to get the folded SFS assuming the reference genome as the ancestral state. We bootstrapped the SFS estimation 300 times.

To estimate the genome-wide nucleotide diversity (π) we first estimated the population-level folded SFS as done with the heterozygosity analysis but providing as input all the samples per group. We calculated per site π directly from each population's SFS in two steps following the approach of Korneliussen et al. (2013) by dividing the pairwise Watterson theta value (Dung et al. 2019; Watterson 1975) over the effective number of sites with data (i.e., including all non-variable sites that passed the filters) per window. We computed these statistics using non-overlapping sliding windows of 50 Kb.

Demography and runs of homozygosity

Genotypes were called with ANGSD from the genotype likelihoods as described above to identify Runs of homozygosity (ROH) in modern individuals with PLINK v1.9 (Purcell et al.

ACCEPTED MANUSCRIPT

Downloaded from https://academic.oup.com/mbe/advance-article/doi/10.1093/molbev/msad256/7442647 by University of Kent user on 27 November 2023

2007). SNPs not in Hardy-Weinberg equilibrium were removed and the remainder SNPs were pruned based on Linkage Disequilibrium (LD) $r^2 > 0.8$ as implemented in Foote et al. (2021). The following parameters were used to estimate ROHs: minimum window size = 10 SNPs, minimum density per 50 kb = 1 SNP, maximum heterozygous sites per window = 5, and a maximum distance between SNPs = 1000 kb.

Analysis of recent (<100 generations) demography was performed with GONE (Santiago et al. 2020) which uses the patterns of LD to estimate recent population size changes. We used unphased genotypes of the modern samples as described for the ROHs and assumed a recombination rate of 3 cM/Mb with 40 replicates and default parameters. In order to have an estimate of the bias and variance of the results, we did a jackknife cross-validation by sampling out one individual at a time and computing the demography with GONE at each iteration.. No subsampling of SNPs was needed as none of the 148 used scaffolds exceeded the 100,000 upper limit of GONE. A total of 1,368,272 genome-wide SNPs were used in each iteration.

Long-term (>5,000 generations) demography analysis was calculated with PSMC (Li and Durbin 2011) using the publicly available reference genome that was sequenced to a depth of coverage of 75x. The consensus diploid sequence was computed using SAMTOOLS and bcftools (Danecek et al. 2021). The settings for the PSMC were as follows: -N30 -t5 -r5 -p "4+30*2+4+6+10" following Nadachowska-Brzyska et al. (2015). A total of 100 independent bootstrap rounds were combined and the final plot was generated assuming a mutation rate of 4.6e-9 (as reported in the collared flycatcher; Smeds et al. 2016) and a generation time of 2 years (R Bristol, unpublished data).

Genetic load analyses

We individually called high-quality SNPs in each of the historical and modern individuals with bcftools (Danecek et al. 2021) to produce a gvcf file (i.e. including invariant sites), retaining all sites with a minimum base and mapping quality of 30, a minimum depth of 4X and a maximum of 34X, and ignoring InDels and their surrounding SNPs (5 bp). We individually annotated each filtered SNP file with SNPeff v.4.3. (Cingolani et al. 2012) using a custom database with our annotated reference genome. We classified putatively deleterious variants into three categories (i) Low-impact variants that are likely to be not deleterious (i.e., synonymous), (ii) Moderate-impact variants that are likely to modify the protein effectiveness (i.e., missense), and (iii) High-impact variants are likely to disrupt the protein function (i.e. loss of function LoF) (Cingolani et al. 2012). We merged the annotated gvcf files and retained only variants with less than 30% missing data and whose derived alleles were present in at least one individual of each of the

ACCEPTED MANUSCRIPT

Downloaded from https://academic.oup.com/mbe/advance-article/doi/10.1093/molbev/msad256/7442647 by University of Kent user on 27 November 2023

historical and modern timepoints. To identify which allelic states were likely ancestral, we extracted the reconstructed sequence of the ancestral node that contains our target species based on an alignment of 363 bird assemblies from Feng et al. (2020) and mapped it to our reference genome with the default parameters of BWA mem (Li and Durbin 2009). This node contains three sister species; *Myiagra hebetior* (estimated divergence time 12 MYA), *Paradisaea raggiana* and *Ifrita kowaldi* (estimated divergence time 25 MYA) (Jønsson et al. 2016; Kumar et al. 2022), and was assumed to represent the ancestral allele state. We randomly iterate over this dataset at two levels. First, to account for the variation due to different samples sizes between timepoints we randomly subsampled (with replacement) modern individuals to the same sample size as historical ones (N=13). Second, to account for variation across the genome we randomly choose 1000 filtered variants in each iteration. Sites and individuals were randomly sampled this way 100 times.

In each iteration, we tested (1) if there was a variant frequency difference between historical and modern samples, and (2) if historical and modern individuals had different number of deleterious alleles. (1) We estimated the relative frequency of putative deleterious variants between historical and modern time points per category using the R_{xy} approach described in Xue et al. (2015) following Dussex et al. 2021. Briefly, we estimated the per-site derived allele frequencies per timepoints ($sFreq_{hist}$ and $sFreq_{mod}$) and calculated the per-category frequency as $cFreq_{hist} = \sum sFreq_{hist}(1- sFreq_{mod})$ and vice versa. We then estimated $R_{xy} = cFreq_{hist}/ cFreq_{mod}$, where a value of 1 corresponds to no change in frequency, a value higher than 1 represents a deficit in the modern population, and a value lower than 1 represents an increase in the modern population. (2) We counted the total number of derived alleles per site per individual, and the count of those in homozygous state. The total count approximates the total genetic load in a sample, including mutations that do not express fitness effects (i.e., masked load) and those that fully or partially express their fitness effect (i.e., realised load). The homozygous counts approximate most of the realised load because these mutations fully express their deleterious effects. Partially recessive (heterozygous) deleterious mutations are also expected to partially express their deleterious effects, and thus being part of the realised load (Bertorelle et al. 2022). However, dominance coefficients (*h*) of mildly and highly deleterious mutations are likely to be mostly recessive (Charlesworth and Willis 2009; Fig. S19) and thus are mostly part of the masked load (Bertorelle et al. 2022). Since the historical and modern samples have different sequence quality that impacts our ability to call SNPs, we corrected these derived allelic counts by dividing them by the total count of derived synonymous sites (i.e., low-impact variants), following Kuang et al. (2020). For each the allele count comparison (across all iterations) we

ACCEPTED MANUSCRIPT

Downloaded from https://academic.oup.com/mbe/advance-article/doi/10.1093/molbev/msad256/7442647 by University of Kent user on 27 November 2023

tested if the difference between historical and modern individuals was significant with the function t-test in R.

Individual-based simulations

We performed individual-based forward simulations with SLiM v3.6 (Haller and Messer 2019) with a non-Wright-Fisher implementation. Absolute fitness (i.e., probability of survival) was regulated by genetic effects (see below) and the carrying capacity, which was determined with the reconstructed pre-bottleneck population size (see Results) and the known trajectory of the population decline and recovery (Bristol et al. 2013). We implemented three scenarios with different ancestral population sizes starting from the estimated ancestral population size, and population sizes that were 5 and 10 times larger (i.e., 1X, 5X or 10X). We ran a burn-in for a number of generations that was five times the population size to obtain an ancestral population in mutation-selection-drift equilibrium. We ran 100 replicates per scenario.

To confirm that our model successfully replicated the overall biology of the Seychelles paradise flycatcher, we parameterised the model with known distributions for age-based mortality probability and litter size (Currie et al. 2005). We then analysed the resulting full genealogy (with Tree sequence recording; Haller et al. 2019) to estimate the emerging generation time in the simulation, which matched the known generation time of ~2 years in this species (R. Bristol unpublished data).

Genetics parameters: we simulated 10,000 genes of 1 Kb each distributed across 28 autosomal chromosomes, typical of a passerine genome. We used a recombination rate of 1e-4 per base position, per generation, with no recombination within genes. We use a relatively large mutation rate of 1e-7 per bp to compensate for the small, simulated genome size and ensure the accumulation of genetic load in the ancestral populations.

To investigate the effect of the genetic load, we simulated deleterious mutations. We first investigated the relationship between selection (s) and dominance (h) coefficients in the distribution of fitness effects (DFE). For this, we conducted simulations with unconstrained mutations (Fig. S19; DFE0 in Fig. S20). Specifically, we drew values of s and h from uniform distributions ($-1<s<0$ and $0.5<h< 0$), allowing any combination of s and h to occur. Natural selection acts on this variation and a gamma distribution of DFE with a negative relationship between h and s naturally emerges from the simulations (Fig. S19). We randomly sampled 10,000 mutations in each replicate from the resulting simulated DFE to parametrise our simulations. Deleterious mutations appeared at a ratio of 2.31:1 relative to neutral mutations as observed in human exons (Kim et al. 2017). This distribution is approximately consistent with

ACCEPTED MANUSCRIPT

Downloaded from https://academic.oup.com/mbe/advance-article/doi/10.1093/molbev/msad256/7442647 by University of Kent user on 27 November 2023

the predicted DFE of deleterious variation in humans (Eyre-Walker and Keightley 2007) meta-analysis (Charlesworth and Willis 2009) and experimental approaches (Agrawal and Whitlock 2012). Furthermore, we tested alternative DFEs previously used elsewhere (Kardos et al. 2021; Kyriazis et al. 2021; Pérez-Pereira et al. 2021; DFE1-DFE4 in Fig. S20) to compare the resulting trajectories of genetic load and probability of extinction over time (Figs. S20-S21)

To investigate the effect of adaptive potential, we simulated the additive effect of genotype values (*z*) on a polygenic trait tracking an environmental optimum (*opt*). Genotype values (*z*) were drawn from a uniform distribution, and with a fixed additive effect (*h*=0.5). The effect of homozygous loci was estimated as Σz, the effect of the heterozygous loci as Σzh, and the phenotype (*P*) of an individual was the sum of the homozygous and heterozygous effects. Following Falconer and Mackay (1996), we calculated the fitness effect from the deviation of the phenotype to the environmental optimum as $w = (P - opt)^2$ and the additive genetic variation as $V_A = \Sigma 2 p_i q_i {z_i}^2$. We performed an extensive parameter space exploration to test the effect of (i) the range from which genotype values (z) were drawn for the polygenic trait, and (ii) the relative proportion of mutation contributing to the adaptive trait relative to those contributing to the genetic load (Figs. S22-S24). In the main text and Fig. 4, we present the results for simulations that take their genotype values (z) from uniform distribution ranging between -0.25 to 0.25 and with a proportion of 0.2 of mutation contributing to the adaptive trait relative to those contributing to the genetic load.

Acknowledgments

We are grateful to curators Hein van Grouw from the Natural History Museum, Tring, UK and Michael Brooke from the Museum of Zoology, University of Cambridge, UK. Darwin Initiative grant 15/009 to JG facilitated blood-sampling of the modern population. We are grateful to members of the B10K consortium for their work on the reference genome and Ester Milesi for help processing samples. We thank Shyam Gopalakrishnan and Xin Sun for bioinformatics advice. GF was supported by UNAM-DGECI *Iniciación a la Investigación*. CvO was funded by the Earth and Life Systems Alliance (ELSA). MTPG acknowledges DNRF143 award for funding. HEM was funded by the European Union's Horizon 2020 Research and Innovation Programme under a Marie Sklodowska-Curie grant (840519) and by the ERC (ERODE, 101078303). Views and opinions expressed are those of the authors only and do not necessarily reflect those of the European Union or the European Research Council. Neither the European Union nor the granting authority can be held responsible for them.

ACCEPTED MANUSCRIPT

Downloaded from https://academic.oup.com/mbe/advance-article/doi/10.1093/molbev/msad256/7442647 by University of Kent user on 27 November 2023

Data availability

The reference genome can be found at https://b10k.scifeon.cloud/#/b10k/Sample/S15237. The raw sequencing reads have been deposited in the Sequence Read Archive under the accession number PRJNA922178. Scripts can be found at https://github.com/hmoral/SPF

Author contributions

HEM, MTPG and JG conceived the study. GF generated the data. GF and HEM performed the analysis. CvO and JG provided insights to interpret the result. JG and RMB provided samples and insights about the study species. HEM and MTPG provided resources. GZ and SF developed the reference genome. HEM wrote the manuscript with the assistance of GF, CvO and MTPG. All authors provided feedback and approved the final version.

Legends

Figure 1. The Seychelles paradise flycatcher shows a massive loss of genome-wide diversity after population decline and despite its demographic recovery. (A) Whole-genome sequencing from historical (over 130-year-old - circles; La Digue, orange and Praslin, purple) and modern (triangles; La Digue, green) individuals. The inset shows the species' recent demographic trajectory estimated by (Bristol et al. 2013) showing the dramatic population decline and subsequent recovery. (B) Principal component analysis of historical and modern samples. (C) On average, modern individuals have 6.4 times less observed heterozygosity than historical individuals. (D) On average, the modern population has 10.9 times less nucleotide diversity than the historical populations, and diversity was lost uniformly through the genome (here we show the longest four scaffolds; the rest of the scaffolds can be found in Fig. S14). The reason for the lower π in Praslin is that pairwise nucleotide diversity is sensitive to the population sample size and the precision power gained from a larger sample size in La Digue; this effect is not seen in the individual average heterozygosity (panel C).

Figure 2. Demographic reconstruction of population decline. (A) Runs of homozygosity (ROH) length distribution across all modern individuals. (B) Inbreeding coefficient estimated for different classes of ROH lengths (F_{ROH}). The year represents the estimated time at which a category of ROH length was formed assuming a recombination rate of 3 cM/Mb and using the formula L = 100/2t cM from (Thompson 2013), where *L* is the ROH length and *cM* is the recombination rate, to obtain *t* the time of ROH coalescence in generations. Generations ago were converted assuming a generation time of 2 years from the time of sampling. (C) Reconstruction of the recent demography (last 100 generations) from Linkage Disequilibrium using GONE (Santiago et al. 2020) assuming a recombination rate of 3 cM/Mb. Light-grey lines were obtained with a jackknife approach removing one sample at a time, the red line is the mean across replicates. Generations ago were converted assuming a generation time of 2 years from the time of sampling (2010). (D) Reconstruction of the ancient demography (<10,000 years ago or 5,000 generations ago) from genetic coalescence using PSMC (Li and Durbin 2011) assuming a mutation rate of 2.3e-9 and a generation time of 2 years.

ACCEPTED MANUSCRIPT

Downloaded from https://academic.oup.com/mbe/advance-article/doi/10.1093/molbev/msad256/7442647 by University of Kent user on 27 November 2023

Figure 3. Genetic load dynamics over time. (A) Allelic frequency differential between modern and historical samples (Rxy) for three categories of putative deleterious mutations. Values equal to one indicate no frequency difference, values below one indicate a higher frequency in the modern population, and values in excess of one a lower frequency in the modern population. Synonymous (mean= 0.71; 95%CI=0.7-0.72), and missense (mean= 0.76; 95%CI=0.75-0.77) have significantly increased in frequency in the modern samples ($p<0.001$), and loss-of-function (LoF) mutations (mean= 1.21; 95%CI=1.16-1.25) have significantly decreased in frequency ($p<0.001$). (B) Total count of derived alleles in modern and historical individuals for missense and LoF mutation normalized by the count of derived synonymous alleles. There is no significant difference between historical and modern individuals counts of LoF alleles (difference = -2.7e-04, 95% CI [-4.4e-04, 9.9e-04], t = 0.75, p = 0.45). Modern individuals have a significant higher count of missense alleles (difference = 0.07, 95% CI [0.07, 0.07], t = 47.7, p < 0.001). (C) Count of homozygous derived alleles in modern and historical individuals for missense and LoF mutation normalized by the count of derived synonymous alleles. There is a very small, but statistically significant, reduction in the homozygous derived counts of LoF alleles in the modern individuals (difference = -2.2e-03, 95% CI [-2.9e-03, -1.6e-03], t = -6.74, p < .001). In contrast, modern individuals have a significant higher count of missense alleles (difference = 0.03, 95% CI [0.02, 0.03], t = 21.32, p < 0.001).

Figure 4. Forward simulations of deleterious and adaptive variation. (A) Alternative simulated demographic trajectories. The 1X trend (red) represents the known ancestral size of the Seychelles paradise flycatcher based on the reconstruction of the recent demography with GONE (Fig. 2C). The alternative scenarios represent medium (5X, yellow) and large (10X, blue) ancestral population sizes. The trajectory was divided into six stages: Ancestral (years 1810-1815), Collapse (1965-1970), Recovery (1990-1995), Present (2010-2015), Environmental change (2050-2055), Future (2095-2100). During the environmental shift, the quantitative trait optimum value moved from 0.2 to 1.2, resulting in a loss of fitness followed by adaptive evolutionary change. (B) Genetic load. (C) Masked load. (D) Realised load. We calculated the genetic load components, following Bertorelle et al. (2022): $Genetic\ load = \sum_{i=1}^{L} q_i\, s_i$, $Realised\ load = \sum_{i=1}^{L} q_i^2 s_i + 2\sum_{i=1}^{L} q_i [1 - q_i] h_i s_i$, and masked load = genetic load – realised load. Furthermore, s_i is the selection coefficient, h_i the dominance coefficient, and q_i the frequency of the mutation at loci L. The genetic load, masked load and realised load are all in lethal equivalents (see Bertorelle et al. 2022). The reduction in fitness (w) due to the expression of unconditionally deleterious mutations (i.e., inbreeding depression) is a function of the realised load: $w = e^{-\text{Realised Load}}$. (E) Extinction probability per scenario (the number of surviving replicates divided by the total number of replicates). (F) Additive genetic variance in the quantitative trait. (G) Fitness effect conferred by the quantitative trait.

References

Agrawal AF, Whitlock MC. 2012. Mutation Load: The Fitness of Individuals in Populations Where Deleterious Alleles Are Abundant. *Annu. Rev. Ecol. Evol. Syst.* 43:115–135.

Ali JR. 2018. Islands as biological substrates: Continental. *J. Biogeogr.* 45:1003–1018.

Almond REA, Grooten M, Peterson T. 2022. Living Planet Report 2020-Bending the curve of biodiversity loss. Available from: http://pure.iiasa.ac.at/id/eprint/16870/1/ENGLISH-FULL.pdf

Broad Institute. 2018. Picard. Available from: http://broadinstitute.github.io/picard/

Andrews S. 2010. FastQC: A quality control analysis tool for high throughput sequencing data. Babraham Institute Available from: https://www.bioinformatics.babraham.ac.uk/projects/fastqc/

Barthe M, Doutrelant C, Covas R, Melo M, Illera JC, Tilak M-K, Colombier C, Leroy T, Loiseau C, Nabholz

ACCEPTED MANUSCRIPT

Downloaded from https://academic.oup.com/mbe/advance-article/doi/10.1093/molbev/msad256/7442647 by University of Kent user on 27 November 2023

B. 2022. Evolution of immune genes in island birds: reduction in population sizes can explain island syndrome. *Peer Community Journal* [Internet] 2. Available from: https://peercommunityjournal.org/articles/10.24072/pcjournal.186/
Behr AA, Liu KZ, Liu-Fang G, Nakka P, Ramachandran S. 2016. pong: fast analysis and visualization of latent clusters in population genetic data. *Bioinformatics* 32:2817–2823.
Bellinger MR, Johnson JA, Toepfer J, Dunn P. 2003. Loss of genetic variation in greater prairie chickens following a population bottleneck in Wisconsin, U.s.a. *Conserv. Biol.* 17:717–724.
Bertorelle G, Raffini F, Bosse M, Bortoluzzi C, Iannucci A, Trucchi E, Morales HE, van Oosterhout C. 2022. Genetic load: genomic estimates and applications in non-model animals. *Nat. Rev. Genet.* 23:492–503.
Boitard S, Arredondo A, Chikhi L, Mazet O. 2022. Heterogeneity in effective size across the genome: effects on the inverse instantaneous coalescence rate (IICR) and implications for demographic inference under linked selection. *Genetics* [Internet] 220. Available from: http://dx.doi.org/10.1093/genetics/iyac008
Bozzuto C, Biebach I, Muff S, Ives AR, Keller LF. 2019. Inbreeding reduces long-term growth of Alpine ibex populations. *Nature Ecology & Evolution* [Internet] 3:1359–1364. Available from: http://dx.doi.org/10.1038/s41559-019-0968-1
Bristol RM. 2014. Conservation of the Seychelles paradise flycatcher. Available from: https://kar.kent.ac.uk/id/eprint/100278
Bristol RM, Tucker R, Dawson DA, Horsburgh G, Prys-Jones RP, Frantz AC, Krupa A, Shah NJ, Burke T, Groombridge JJ. 2013. Comparison of historical bottleneck effects and genetic consequences of re-introduction in a critically endangered island passerine. *Mol. Ecol.* 22:4644–4662.
Charlesworth B. 2013a. Why we are not dead one hundred times over. *Evolution* 67:3354–3361.
Charlesworth B. 2013b. Stabilizing selection, purifying selection, and mutational bias in finite populations. *Genetics* 194:955–971.
Charlesworth D, Willis JH. 2009. The genetics of inbreeding depression. *Nat. Rev. Genet.* 10:783–796.
Cheke AS, Hume JP. 2008. Lost land of the Dodo: the ecological history of the Mascarene Islands. *T and AD Poyser, London*.
Cingolani P, Platts A, Wang LL, Coon M, Nguyen T, Wang L, Land SJ, Lu X, Ruden DM. 2012. A program for annotating and predicting the effects of single nucleotide polymorphisms, SnpEff: SNPs in the genome of Drosophila melanogaster strain w1118; iso-2; iso-3.
Currie D, Bristol R, Millett J, Shah NJ. 2005. Demography of the Seychelles Black Paradise-flycatcher: considerations for conservation and reintroduction. *Ostrich* 76:104–110.
Danecek P, Bonfield JK, Liddle J, Marshall J, Ohan V, Pollard MO, Whitwham A, Keane T, McCarthy SA, Davies RM, et al. 2021. Twelve years of SAMtools and BCFtools. Gigascience 10: giab008.
Díez-del-Molino D, Sánchez-Barreiro F, Barnes I, Gilbert MTP, Dalén L. 2018. Quantifying Temporal Genomic Erosion in Endangered Species. *Trends Ecol. Evol.* 33:176–185.
Dung SK, López A, Barragan EL, Reyes R-J, Thu R, Castellanos E, Catalan F, Huerta-Sánchez E, Rohlfs RV. 2019. Illuminating Women's Hidden Contribution to Historical Theoretical Population Genetics. *Genetics* 211:363–366.
Dussex N, van der Valk T, Morales HE, Wheat CW, Díez-del-Molino D, von Seth J, Foster Y, Kutschera VE, Guschanski K, Rhie A, et al. 2021. Population genomics of the critically endangered kākāpō. *Cell Genomics* 1:100002.
Dussex, N., Morales, H. E., Grossen, C., Dalén, L., & van Oosterhout, C. (2023). Purging and accumulation of genetic load in conservation. Trends in Ecology & Evolution.
Ebenesersdóttir SS, Sandoval-Velasco M, Gunnarsdóttir ED, Jagadeesan A, Guðmundsdóttir VB, Thordardóttir EL, Einarsdóttir MS, Moore KHS, Sigurðsson Á, Magnúsdóttir DN, et al. 2018. Ancient genomes from Iceland reveal the making of a human population. *Science* 360:1028–1032.
Ewels P, Magnusson M, Lundin S, Käller M. 2016. MultiQC: summarize analysis results for multiple tools and samples in a single report. *Bioinformatics* 32:3047–3048.
Eyre-Walker A, Keightley PD. 2007. The distribution of fitness effects of new mutations. *Nat. Rev. Genet.* 8:610–618.
Fabre P-H, Moltensen M, Fjeldså J, Irestedt M, Lessard J-P, Jønsson KA. 2014. Multiple waves of colonization by monarch flycatchers (Myiagra , Monarchidae) across the Indo-Pacific and their implications for coexistence and speciation. *J. Biogeogr.* 41:274–286.
Fagan WF, Holmes EE. 2006. Quantifying the extinction vortex. *Ecol. Lett.* 9:51–60.

ACCEPTED MANUSCRIPT

Downloaded from https://academic.oup.com/mbe/advance-article/doi/10.1093/molbev/msad256/7442647 by University of Kent user on 27 November 2023

Falconer DS, Mackay TFC. Introduction to quantitative genetics 4th edition. *Harlow, UK: Longmans*.
Feng S, Fang Q, Barnett R, Li C, Han S, Kuhlwilm M, Zhou L, Pan H, Deng Y, Chen G, et al. 2019. The Genomic Footprints of the Fall and Recovery of the Crested Ibis. *Curr. Biol.* 29:340–349.e7.
Feng, S., Stiller, J., Deng, Y., Armstrong, J., Fang, Q. I., Reeve, A. H., ... & Zhang, G. (2020). Dense sampling of bird diversity increases power of comparative genomics. Nature, 587(7833), 252-257.
Foote AD, Hooper R, Alexander A, Baird RW, Baker CS, Ballance L, Barlow J, Brownlow A, Collins T, Constantine R, et al. 2021. Runs of homozygosity in killer whale genomes provide a global record of demographic histories. *Mol. Ecol.* 30:6162–6177.
Forester BR, Beever EA, Darst C, Szymanski J, Funk WC. 2022. Linking evolutionary potential to extinction risk: applications and future directions. *Front. Ecol. Environ.* 20:507–515.
García-Dorado, A. 2012. Understanding and predicting the fitness decline of shrunk populations: inbreeding, purging, mutation, and standard selection. *Genetics* 190:1461–1476.
Garcia-Erill G, Albrechtsen A. 2020. Evaluation of model fit of inferred admixture proportions. *Mol. Ecol. Resour.* 20:936–949.
Gilroy DL, Phillips KP, Richardson DS, van Oosterhout C. 2017. Toll-like receptor variation in the bottlenecked population of the Seychelles warbler: computer simulations see the “ghost of selection past” and quantify the “drift debt.” *J. Evol. Biol.* 30:1276–1287.
Ginolhac A, Rasmussen M, Gilbert MTP, Willerslev E, Orlando L. 2011. mapDamage: testing for damage patterns in ancient DNA sequences. *Bioinformatics* 27:2153–2155.
Gopalakrishnan S, Ebenesersdóttir SS, Lundstrøm IKC, Turner-Walker G, Moore KHS, Luisi P, Margaryan A, Martin MD, Ellegaard MR, Magnússon ÓÞ, et al. 2022. The population genomic legacy of the second plague pandemic. *Curr. Biol.* [Internet]. Available from: http://dx.doi.org/10.1016/j.cub.2022.09.023
Grilz-Seger G, Mesarič M, Cotman M, Neuditschko M, Druml T, Brem G. 2018. Runs of Homozygosity and Population History of Three Horse Breeds With Small Population Size. *J. Equine Vet. Sci.* 71:27–34.
Groombridge JJ, Jones CG, Bayes MK, van Zyl AJ, Carrillo J, Nichols RA, Bruford MW. 2002. A molecular phylogeny of African kestrels with reference to divergence across the Indian Ocean. *Mol. Phylogenet. Evol.* 25:267–277.
Grossen C, Guillaume F, Keller LF, Croll D. 2020. Purging of highly deleterious mutations through severe bottlenecks in Alpine ibex. *Nat. Commun.* 11:1001.
Haller BC, Galloway J, Kelleher J, Messer PW, Ralph PL. 2019. Tree-sequence recording in SLiM opens new horizons for forward-time simulation of whole genomes. *Mol. Ecol. Resour.* 19:552–566.
Haller BC, Messer PW. 2019. SLiM 3: Forward Genetic Simulations Beyond the Wright–Fisher Model. *Mol. Biol. Evol.* 36:632–637.
Hanghøj K, Moltke I, Andersen PA, Manica A, Korneliussen TS. 2019. Fast and accurate relatedness estimation from high-throughput sequencing data in the presence of inbreeding. *Gigascience* [Internet] 8. Available from: http://dx.doi.org/10.1093/gigascience/giz034
Hansson B, Westerberg L. 2002. On the correlation between heterozygosity and fitness in natural populations. *Mol. Ecol.* 11:2467–2474.
Harrisson KA, Pavlova A, Telonis-Scott M, Sunnucks P. 2014. Using genomics to characterize evolutionary potential for conservation of wild populations. *Evol. Appl.* 7:1008–1025.
Hedrick PW, Garcia-Dorado A. 2016. Understanding Inbreeding Depression, Purging, and Genetic Rescue. *Trends Ecol. Evol.* 31:940–952.
Henriette E, Laboudallon V. 2011. Seychelles paradise flycatcher conservation introduction: population assessment on Denis Island, Seychelles. *Unpublished report*.
Hoban S, Bruford M, D’Urban Jackson J, Lopes-Fernandes M, Heuertz M, Hohenlohe PA, Paz-Vinas I, Sjögren-Gulve P, Segelbacher G, Vernesi C, et al. 2020. Genetic diversity targets and indicators in the CBD post-2020 Global Biodiversity Framework must be improved. *Biol. Conserv.* 248:108654.
IUCN. 2022. IUCN Red List of Threatened Species. *IUCN Red List of Threatened Species* [Internet]. Available from: https://www.iucnredlist.org
Jensen EL, Díez-Del-Molino D, Gilbert MTP, Bertola LD, Borges F, Cubric-Curik V, de Navascués M, Frandsen P, Heuertz M, Hvilsom C, et al. 2022. Ancient and historical DNA in conservation policy. *Trends Ecol. Evol.* 37:420–429.
Johri P, Riall K, Becher H, Excoffier L, Charlesworth B, Jensen JD. 2021. The Impact of Purifying and Background Selection on the Inference of Population History: Problems and Prospects. *Mol. Biol.*

ACCEPTED MANUSCRIPT

Downloaded from https://academic.oup.com/mbe/advance-article/doi/10.1093/molbev/msad256/7442647 by University of Kent user on 27 November 2023

Evol. 38:2986–3003.
Jønsson KA, Fabre P-H, Kennedy JD, Holt BG, Borregaard MK, Rahbek C, Fjeldså J. 2016. A supermatrix phylogeny of corvoid passerine birds (Aves: Corvides). *Molecular Phylogenetics and Evolution* [Internet] 94:87–94. Available from: http://dx.doi.org/10.1016/j.ympev.2015.08.020
Kapp JD, Green RE, Shapiro B. 2021. A Fast and Efficient Single-stranded Genomic Library Preparation Method Optimized for Ancient DNA. *J. Hered.* [Internet] 112. Available from: https://pubmed.ncbi.nlm.nih.gov/33768239/
Kardos M, Armstrong EE, Fitzpatrick SW, Hauser S, Hedrick PW, Miller JM, Tallmon DA, Funk WC. 2021. The crucial role of genome-wide genetic variation in conservation. *Proc. Natl. Acad. Sci. U. S. A.* [Internet] 118. Available from: http://dx.doi.org/10.1073/pnas.2104642118
Khan, A., Patel, K, Shukla, H, Viswanathan, A, van der Valk, ., Borthakur, U, ... & Ramakrishnan, U. 2021. Genomic evidence for inbreeding depression and purging of deleterious genetic variation in Indian tigers. *Proceedings of the National Academy of Sciences*, 118(49), e2023018118.
Kim, BY, Huber CD, & Lohmueller KE. 2017. Inference of the distribution of selection coefficients for new nonsynonymous mutations using large samples. *Genetics* 206:345–361.
Kleinman-Ruiz D, Lucena-Perez M, Villanueva B, Fernández J, Saveljev AP, Ratkiewicz M, Schmidt K, Galtier N, García-Dorado A, Godoy JA. 2022. Purging of deleterious burden in the endangered Iberian lynx. *Proc. Natl. Acad. Sci. U. S. A.* 119:e2110614119.
Kopelman NM, Mayzel J, Jakobsson M, Rosenberg NA, Mayrose I. 2015. Clumpak: a program for identifying clustering modes and packaging population structure inferences across K. *Mol. Ecol. Resour.* 15:1179–1191.
Korneliussen TS, Albrechtsen A, Nielsen R. 2014. ANGSD: Analysis of Next Generation Sequencing Data. *BMC Bioinformatics* 15:356.
Korneliussen TS, Moltke I, Albrechtsen A, Nielsen R. 2013. Calculation of Tajima's D and other neutrality test statistics from low depth next-generation sequencing data. *BMC Bioinformatics* [Internet] 14. Available from: http://dx.doi.org/10.1186/1471-2105-14-289
Kuang W, Hu J, Wu H, Fen X, Dai Q, Fu Q, Xiao W, Frantz L, Roos C, Nadler T, et al. 2020. Genetic Diversity, Inbreeding Level, and Genetic Load in Endangered Snub-Nosed Monkeys (Rhinopithecus). *Front. Genet.* 11:615926.
Kumar S, Suleski M, Craig JM, Kasprowicz AE, Sanderford M, Li M, Stecher G, Hedges SB. 2022. TimeTree 5: An Expanded Resource for Species Divergence Times. *Mol. Biol. Evol.* [Internet] 39. Available from: http://dx.doi.org/10.1093/molbev/msac174
Kuussaari M, Bommarco R, Heikkinen RK, Helm A, Krauss J, Lindborg R, Ockinger E, Pärtel M, Pino J, Rodà F, et al. 2009. Extinction debt: a challenge for biodiversity conservation. *Trends Ecol. Evol.* 24:564–571.
Kyriazis CC, Wayne RK, Lohmueller KE. 2021. Strongly deleterious mutations are a primary determinant of extinction risk due to inbreeding depression. *Evol Lett* 5:33–47.
Labisko J, Bunbury N, Griffiths RA, Groombridge JJ, Chong-Seng L, Bradfield KS, Streicher JW. 2022. Survival of climate warming through niche shifts: Evidence from frogs on tropical islands. *Glob. Chang. Biol.* 28:1268–1286.
Laikre L, Hoban S, Bruford MW, Segelbacher G, Allendorf FW, Gajardo G, Rodríguez AG, Hedrick PW, Heuertz M, Hohenlohe PA, et al. 2020. Post-2020 goals overlook genetic diversity. *Science* 367:1083–1085.
Lande R, Shannon S. 1996. THE ROLE OF GENETIC VARIATION IN ADAPTATION AND POPULATION PERSISTENCE IN A CHANGING ENVIRONMENT. *Evolution* 50:434–437.
Lawson LP, Fessl B, Hernán Vargas F, Farrington HL, Francesca Cunninghame H, Mueller JC, Nemeth E, Christian Sevilla P, Petren K. 2017. Slow motion extinction: inbreeding, introgression, and loss in the critically endangered mangrove finch (Camarhynchus heliobates). *Conserv. Genet.* 18:159–170.
Li H, Durbin R. 2010. Fast and accurate long-read alignment with Burrows-Wheeler transform. *Bioinformatics* 26:589–595.
Li H, Durbin R. 2011. Inference of human population history from individual whole-genome sequences. *Nature* 475:493–496.
Lockwood JL, Cassey P, Blackburn TM. 2009. The more you introduce the more you get: the role of colonization pressure and propagule pressure in invasion ecology. *Divers. Distrib.* 15:904–910.
Lynch M, Conery J, Burger R. 1995. Mutation Accumulation and the Extinction of Small Populations. *Am. Nat.* 146:489–518.

ACCEPTED MANUSCRIPT

Downloaded from https://academic.oup.com/mbe/advance-article/doi/10.1093/molbev/msad256/7442647 by University of Kent user on 27 November 2023

Mable BK. 2019. Conservation of adaptive potential and functional diversity: integrating old and new approaches. *Conserv. Genet.* 20:89–100.
Mallon DP, Jackson RM. 2017. A downlist is not a demotion: Red List status and reality. *Oryx* 51:605–609.
Mathur S, DeWoody JA. 2021. Genetic load has potential in large populations but is realized in small inbred populations. *Evol. Appl.* 14:1540–1557.
Mazet O, Rodríguez W, Grusea S, Boitard S, Chikhi L. 2016. On the importance of being structured: instantaneous coalescence rates and human evolution--lessons for ancestral population size inference?
Meisner J, Albrechtsen A. 2018. Inferring Population Structure and Admixture Proportions in Low-Depth NGS Data. *Genetics* 210:719–731.
Monroe MJ, Butchart SHM, Mooers AO, Bokma F. 2019. The dynamics underlying avian extinction trajectories forecast a wave of extinctions. *Biol. Lett.* 15:20190633.
Nadachowska-Brzyska K, Li C, Smeds L, Zhang G, Ellegren H. 2015. Temporal Dynamics of Avian Populations during Pleistocene Revealed by Whole-Genome Sequences. *Curr. Biol.* 25:1375–1380.
van Oosterhout C, Speak SA, Birley T, Bortoluzzi C, Percival-Alwyn L, Urban LH, Groombridge JJ, Segelbacher G, Morales HE. 2022. Genomic erosion in the assessment of species extinction risk and recovery potential. *bioRxiv* [Internet]:2022.09.13.507768. Available from: https://www.biorxiv.org/content/10.1101/2022.09.13.507768v1
Pečnerová P, Garcia-Erill G, Liu X, Nursyifa C, Waples RK, Santander CG, Quinn L, Frandsen P, Meisner J, Stæger FF, et al. 2021. High genetic diversity and low differentiation reflect the ecological versatility of the African leopard. *Current Biology* [Internet] 31:1862–1871.e5. Available from: http://dx.doi.org/10.1016/j.cub.2021.01.064
Pérez-Pereira N, Pouso R, Rus A, Vilas A, López-Cortegano E, García-Dorado A, Quesada H, Caballero A. 2021. Long-term exhaustion of the inbreeding load in Drosophila melanogaster. *Heredity* 127:373–383.
Pinto, A. V., Hansson, B., Patramanis, I., Morales, H. E., & van Oosterhout, C. (2023). The impact of habitat loss and population fragmentation on genomic erosion. Conservation Genetics, 1-9.
Purcell S, Neale B, Todd-Brown K, Thomas L, Ferreira MAR, Bender D, Maller J, Sklar P, de Bakker PIW, Daly MJ, et al. 2007. PLINK: a tool set for whole-genome association and population-based linkage analyses. *Am. J. Hum. Genet.* 81:559–575.
Robinson JA, Kyriazis CC, Nigenda-Morales SF, Beichman AC, Rojas-Bracho L, Robertson KM, Fontaine MC, Wayne RK, Lohmueller KE, Taylor BL, et al. 2022. The critically endangered vaquita is not doomed to extinction by inbreeding depression. *Science* 376:635–639.
Rocha S, Posada D, Harris DJ. 2013. Phylogeography and diversification history of the day-gecko genus Phelsuma in the Seychelles islands. *BMC Evol. Biol.* 13:3.
Ryan WBF, Carbotte SM, Coplan JO, O'Hara S, Melkonian A, Arko R, Weissel RA, Ferrini V, Goodwillie A, Nitsche F, et al. 2009. Global Multi-Resolution Topography synthesis. *Geochemistry, Geophysics, Geosystems* [Internet] 10. Available from: http://dx.doi.org/10.1029/2008gc002332
Sánchez-Barreiro F, Gopalakrishnan S, Ramos-Madrigal J, Westbury MV, de Manuel M, Margaryan A, Ciucani MM, Vieira FG, Patramanis Y, Kalthoff DC, et al. 2021. Historical population declines prompted significant genomic erosion in the northern and southern white rhinoceros (Ceratotherium simum). *Mol. Ecol.* 30:6355–6369.
Santiago E, Novo I, Pardiñas AF, Saura M, Wang J, Caballero A. 2020. Recent Demographic History Inferred by High-Resolution Analysis of Linkage Disequilibrium. *Mol. Biol. Evol.* 37:3642–3653.
Sax DF, Gaines SD. 2008. Species invasions and extinction: The future of native biodiversity on islands. *Proceedings of the National Academy of Sciences* 105:11490–11497.
Schubert M, Ermini L, Der Sarkissian C, Jónsson H, Ginolhac A, Schaefer R, Martin MD, Fernández R, Kircher M, McCue M, et al. 2014. Characterization of ancient and modern genomes by SNP detection and phylogenomic and metagenomic analysis using PALEOMIX. *Nat. Protoc.* 9:1056–1082.
Schubert M, Ginolhac A, Lindgreen S, Thompson JF, Al-Rasheid KAS, Willerslev E, Krogh A, Orlando L. 2012. Improving ancient DNA read mapping against modern reference genomes. *BMC Genomics* 13:178.
von Seth J, van der Valk T, Lord E, Sigeman H, Olsen R-A, Knapp M, Kardailsky O, Robertson F, Hale M,

ACCEPTED MANUSCRIPT

Downloaded from https://academic.oup.com/mbe/advance-article/doi/10.1093/molbev/msad256/7442647 by University of Kent user on 27 November 2023

Houston D, et al. 2022. Genomic trajectories of a near-extinction event in the Chatham Island black robin. *BMC Genomics* 23:747.
Skotte L, Korneliussen TS, Albrechtsen A. 2013. Estimating individual admixture proportions from next generation sequencing data. *Genetics* 195:693–702.
Smeds L, Ellegren H. 2022. From high masked to high realized genetic load in inbred Scandinavian wolves. *Mol. Ecol.* [Internet]. Available from: http://dx.doi.org/10.1111/mec.16802
Smeds L, Qvarnström A, Ellegren H. 2016. Direct estimate of the rate of germline mutation in a bird. *Genome Res.* 26:1211–1218.
Swaisgood RR, Wang D, Wei F. 2018. Panda Downlisted but not Out of the Woods. *Conserv. Lett.* 11:e12355.
Taylor SS, Jamieson IG, Wallis GP. 2007. Historic and contemporary levels of genetic variation in two New Zealand passerines with different histories of decline. *J. Evol. Biol.* 20:2035–2047.
Thompson EA. 2013. Identity by Descent: Variation in Meiosis, Across Genomes, and in Populations. *Genetics* 194:301–326.
Tilman D, May RM, Lehman CL, Nowak MA. 1994. Habitat destruction and the extinction debt. *Nature* 371:65–66.
Tsai WLE, Schedl ME, Maley JM, McCormack JE. 2020. More than skin and bones: Comparing extraction methods and alternative sources of DNA from avian museum specimens. *Mol. Ecol. Resour.* 20:1220–1227.
Van der Auwera GA, O'Connor BD. 2020. Genomics in the Cloud: Using Docker, GATK, and WDL in Terra. "O'Reilly Media, Inc."
Waples RK, Albrechtsen A, Moltke I. 2019. Allele frequency-free inference of close familial relationships from genotypes or low-depth sequencing data. *Molecular Ecology* [Internet] 28:35–48. Available from: http://dx.doi.org/10.1111/mec.14954
Warren BH, Strasberg D, Bruggemann JH, Prys-Jones RP, Thébaud C. 2010. Why does the biota of the Madagascar region have such a strong Asiatic flavour? *Cladistics* 26:526–538.
Watterson GA. 1975. On the number of segregating sites in genetical models without recombination. *Theor. Popul. Biol.* 7:256–276.
Willi Y, van Buskirk J, Hoffmann AA. 2006. Limits to the Adaptive Potential of Small Populations. *Annu. Rev. Ecol. Evol. Syst.* 37:433–458.
Willi Y, Kristensen TN, Sgrò CM, Weeks AR, Ørsted M, Hoffmann AA. 2022. Conservation genetics as a management tool: The five best-supported paradigms to assist the management of threatened species. *Proc. Natl. Acad. Sci. U. S. A.* [Internet] 119. Available from: http://dx.doi.org/10.1073/pnas.2105076119
Willoughby JR, Sundaram M, Wijayawardena BK, Kimble SJA, Ji Y, Fernandez NB, Antonides JD, Lamb MC, Marra NJ, DeWoody JA. 2015. The reduction of genetic diversity in threatened vertebrates and new recommendations regarding IUCN conservation rankings. *Biol. Conserv.* 191:495–503.
Xue Y, Prado-Martinez J, Sudmant PH, Narasimhan V, Ayub Q, Szpak M, Frandsen P, Chen Y, Yngvadottir B, Cooper DN, et al. 2015. Mountain gorilla genomes reveal the impact of long-term population decline and inbreeding. *Science* 348:242–245.
Zhang G, Rahbek C, Graves GR, Lei F, Jarvis ED, Gilbert MTP. 2015. Genomics: Bird sequencing project takes off. *Nature* 522:34.

ACCEPTED MANUSCRIPT

Downloaded from https://academic.oup.com/mbe/advance-article/doi/10.1093/molbev/msad256/7442647 by University of Kent user on 27 November 2023

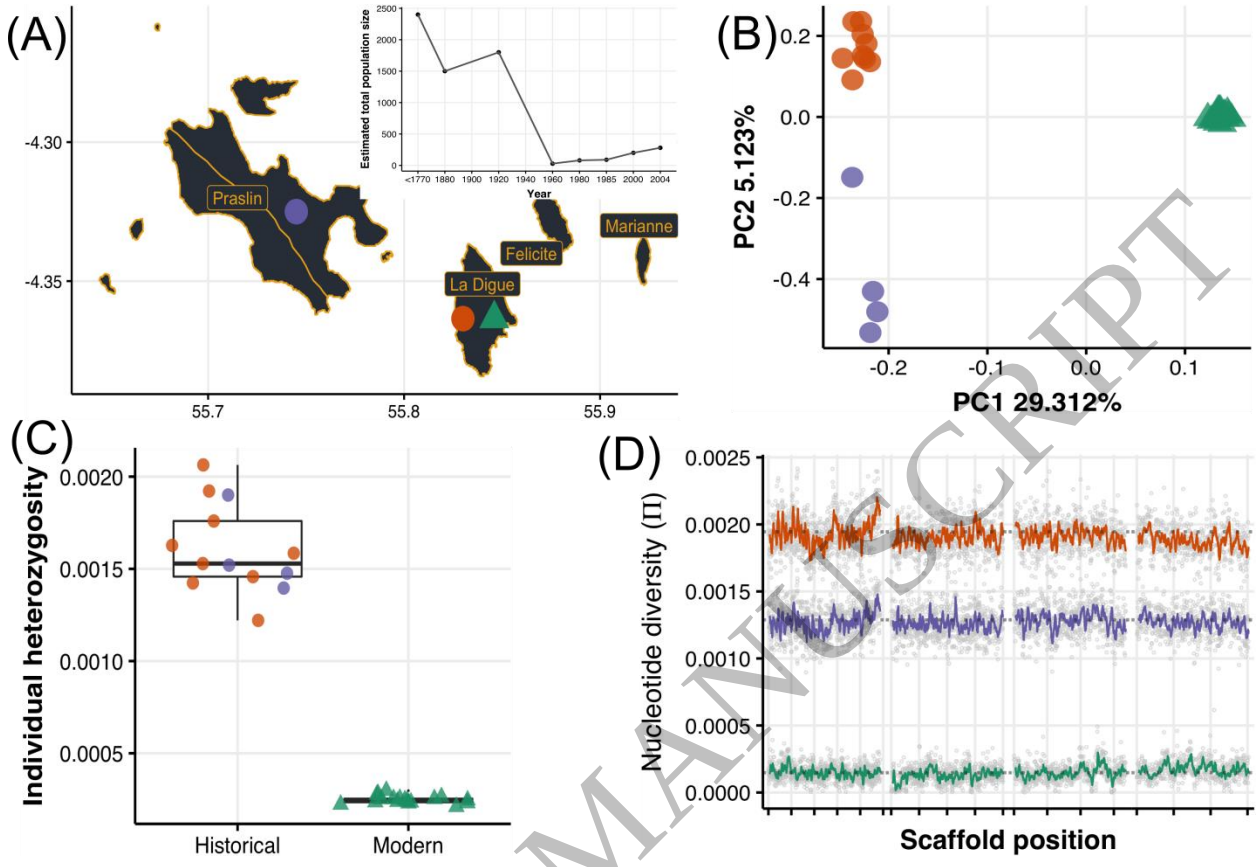
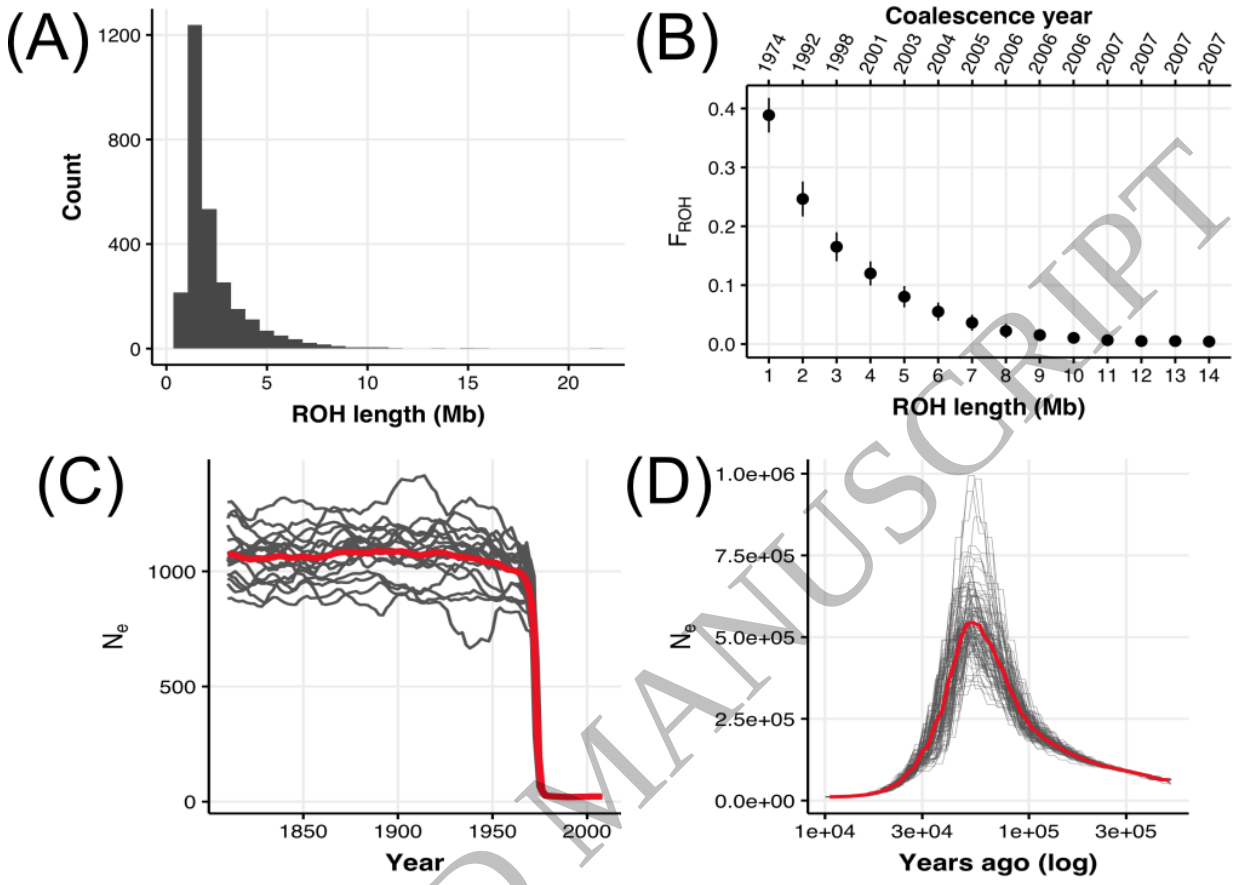


Figure 1

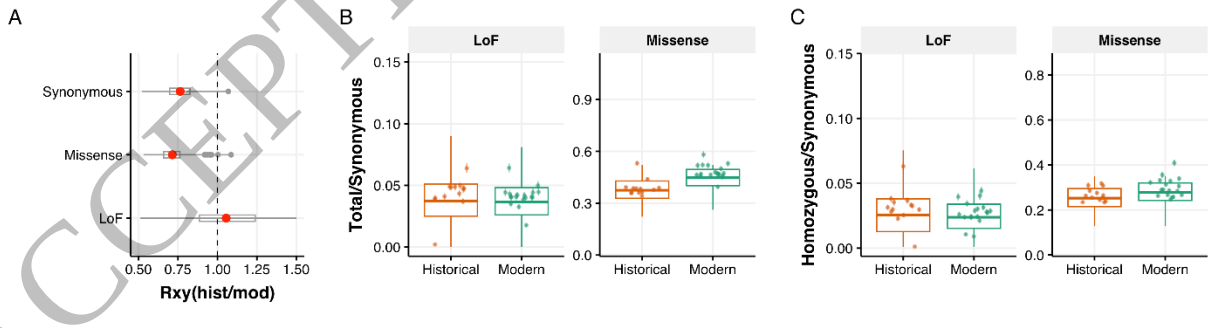
ACCEPTED MANUSCRIPT

Downloaded from https://academic.oup.com/mbe/advance-article/doi/10.1093/molbev/msad256/7442647 by University of Kent user on 27 November 2023



1

2 *Figure 2*



3

4 *Figure 3*

ACCEPTED MANUSCRIPT

Downloaded from https://academic.oup.com/mbe/advance-article/doi/10.1093/molbev/msad256/7442647 by University of Kent user on 27 November 2023

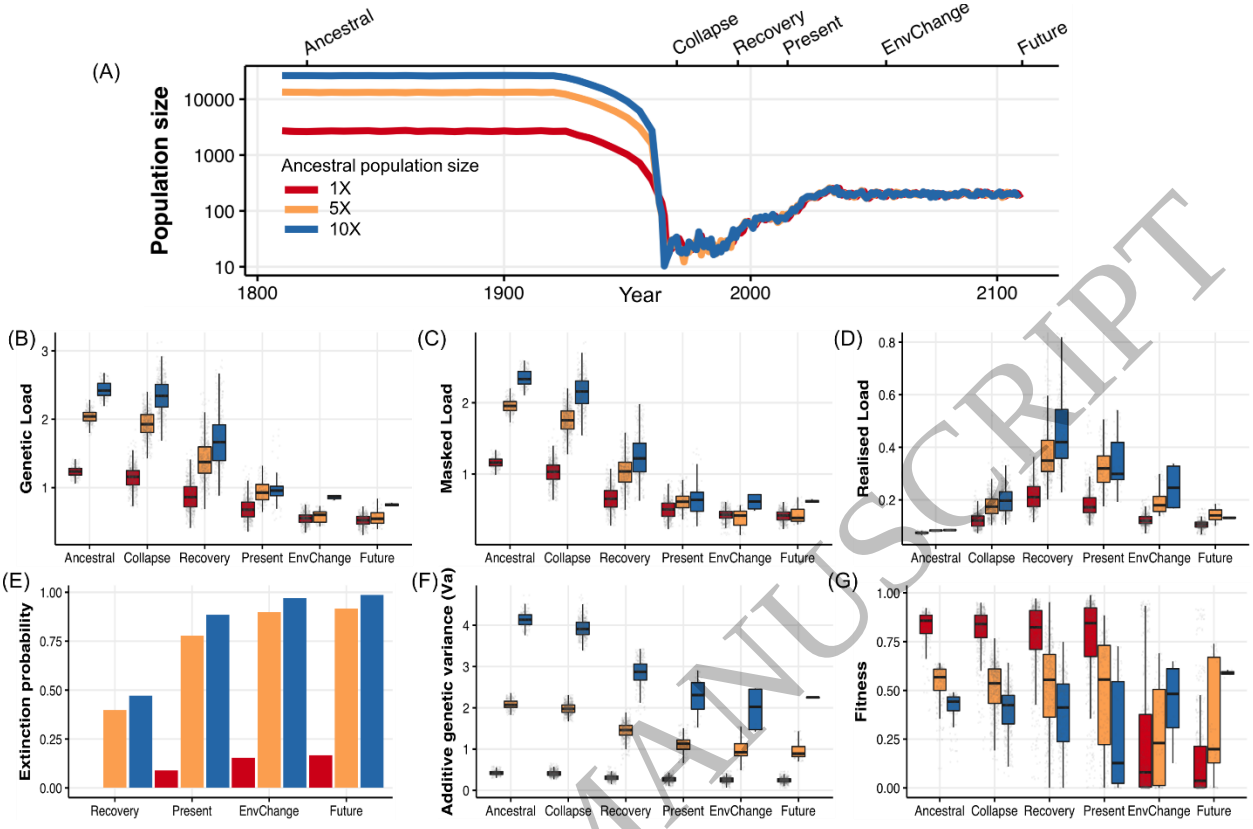


Figure 4

ACCEPTED MANUSCRIPT

Downloaded from https://academic.oup.com/mbe/advance-article/doi/10.1093/molbev/msad256/7442647 by University of Kent user on 27 November 2023